

Field-assisted resonance tunneling through a symmetric double-barrier structure with spin-orbit coupling

Cheng-Zhi Ye,¹ Cun-Xi Zhang,¹ Y.-H. Nie,^{1,2,*} and J.-Q. Liang¹

¹*Institute of Theoretical Physics and Department of Physics, Shanxi University, Taiyuan, Shanxi 030006, China*

²*Department of Physics, Yanbei Normal Institute, Datong, Shanxi 037000, China*

(Received 24 November 2006; revised manuscript received 27 April 2007; published 31 July 2007)

We investigate the electron resonance transmission through a symmetric double-barrier structure with the Dresselhaus spin-orbit coupling and an oscillating field applied to the potential-well region. Based on numerical evaluations, it is demonstrated that the multiphoton process results in a two-set multiplet structure of the transmission spectrum. The number of the resonance peaks and the distance between the adjacent peaks can be controlled by adjusting the amplitude and the frequency of the external field, respectively. Moreover, it is shown that a high spin polarization of the photon-mediated transmission probability can be achieved in the case of narrow potential well with a small amplitude of the oscillating field, which may be useful in the tunable spin filters of high efficiency.

DOI: [10.1103/PhysRevB.76.035345](https://doi.org/10.1103/PhysRevB.76.035345)

PACS number(s): 72.25.Dc, 71.70.Ej, 85.75.Mm

The spin-polarized quantum transport, as a matter of fact, is the theoretic foundation of the spintronic devices. In the past few years, tremendous efforts were devoted to the investigation of the spin-polarized transport in magnetic tunneling junctions and much progress was made both theoretically and experimentally in understanding of the fundamental physics of spintronics.¹⁻³ Recently, the spin-dependent-tunneling phenomena in semiconductor heterostructures have attracted a great deal of attention⁴⁻¹³ and shown the possible application in creating spin injectors and detectors based on nonmagnetic tunneling structures. Spin-dependent tunneling in semiconductor is due to the spin splitting in the electron conductive band which originates from two microscopic mechanisms, Rashba spin-orbit coupling induced by the structural inversion asymmetry^{14,15} and Dresselhaus spin-orbit coupling in noncentrosymmetric materials.¹⁶⁻¹⁸ Spin-orbit interaction couples spin states and space motion of the conductive electrons, which results in the dispersion relation depending on the orientation of electron spin. On the other hand, it was found that in the heterostructures, the electron motion parallel to the tunnel-structure boundary (in-plane motion) can play a well-defined role in the transmission processes because of the discontinuity of the electronic-band parameters at the tunnel-structure interfaces.¹² In asymmetric heterostructures with built-in or external electric fields, coupling between the in-plane electron motion and the electron-spin polarization brings about spin splitting effect through spin-dependent boundary conditions or spin-dependent term in the effective-mass Hamiltonian.^{4,12,19} For symmetric heterostructures with Dresselhaus spin-orbital coupling, in-plane electron motion modifies the effective mass of electron and leads to spin splitting.^{11,20} Spin-dependent transports in semiconductor heterostructures have shown much interesting prospect of technological applications, for example, spin-polarized scanning probe microscopy with an optical orientation of the tunneling electrons,²¹ tunneling spin valves, spin filter,^{5,22} and so on.

Recently, the double barrier has been used to study the spin-dependent resonance tunneling,^{4,11-13} however, without

the Fano resonance. In the asymmetric double-barrier structure induced by an external electric field, the transmission probability depending on the in-plane electron wave vector and the electron-spin polarization is obtained in Ref. 4 and 12 by considering Rashba spin-orbital coupling. Reference 11 is devoted to the spin-dependent tunneling through a symmetric double-barrier structure with Dresselhaus spin-orbital interaction showing the spin-orientation and electron wave-vector dependence of the tunneling probability. Moreover, for the single-barrier-well structure, it is demonstrated that the large spin polarization of the transmission can be obtained using Fano resonance characteristic for energy windows that significantly exceed the spin splitting,^{20,30} where the Fano resonance is induced by the quasibound state in the X valley of the semiconductor.^{20,30} In this paper, we investigate the photon-mediated resonance tunneling of the electron through a symmetric semiconductor double-barrier structure with Dresselhaus spin-orbit coupling and an oscillating field confined in the potential-well region. The potential well provides the bound-state channel of transport inducing the Fano resonance. The advantage of our device compared with the indirect barrier tunneling³⁰ is that the Fano resonance is controllable by the external field. A multiplet structure of the transmission spectrum occurs because of the multiphoton process. The number of the resonance peaks in the multiplet spectrum and the distance between the adjacent peaks can be controlled by adjusting the amplitude and the frequency of the external field, respectively. The combination of spin-orbit coupling and in-plane wave vector makes the multiplet spectrum splitting into two sets, which may be used to modulate the spin polarization of the transmission electron. For a narrow potential well, the large spin polarization occurs in the energy windows whose width can be properly controlled by the applied field, which is useful in the tunable spin filter of high efficiency.

We consider the transmission of a single electron with incident wave vector $k=(k_{\parallel},k_z)$ through a symmetrical double-barrier structure along the $z\parallel[001]$ direction with an oscillating field confined in the potential-well region expressed as

$$V(z,t) = \begin{cases} 0, & z \leq -b \text{ and } z \geq a+b \\ -V_0 + V_1 \cos(\omega t), & 0 \leq z \leq a \\ V_m, & -b < z < 0 \text{ and } a < z < a+b, \end{cases} \quad (1)$$

where V_0 is the static well depth and V_1 and ω denote the amplitude and frequency of the applied field, respectively. V_m is the barrier height depending on the practical semiconductor material. k_{\parallel} is the wave vector parallel to the barrier plane (i.e., in-plane wave vector), and k_z is the wave vector perpendicular to the barrier plane along the direction of tunneling. In this paper, we consider the five-layer semiconductors GaAs/Ga_{0.7}Al_{0.3}As/GaSb/Ga_{0.7}Al_{0.3}As/GaAs. A single electron incident from the left passes five regions denoted by I, II, III, IV, and V (see Fig. 1). We assume the low enough temperature so that the electron-phonon interaction can be neglected. Thus, the electron motion can be described by a time-dependent Schrödinger equation,

$$i\hbar \frac{\partial}{\partial t} \Phi = \hat{H} \Phi, \quad (2)$$

with the effective-mass approximation Hamiltonian

$$\hat{H} = -\frac{\hbar^2}{2\mu_i} \frac{\partial^2}{\partial z^2} + \frac{\hbar^2 k_{\parallel}^2}{2\mu_i} + V(z,t) + \hat{H}_D \quad (i=1,2,3). \quad (3)$$

Here, μ_1 , μ_2 , and μ_3 are, respectively, the effective masses of the electron for materials GaAs, Ga_{0.7}Al_{0.3}As, and GaSb. \hat{H}_D describes the Dresselhaus spin-orbit coupling in zincblende structure. Assuming that the kinetic energy of incident electron is much smaller than the potential-well depth V_0 , the Dresselhaus term \hat{H}_D may be expressed as^{10,11}

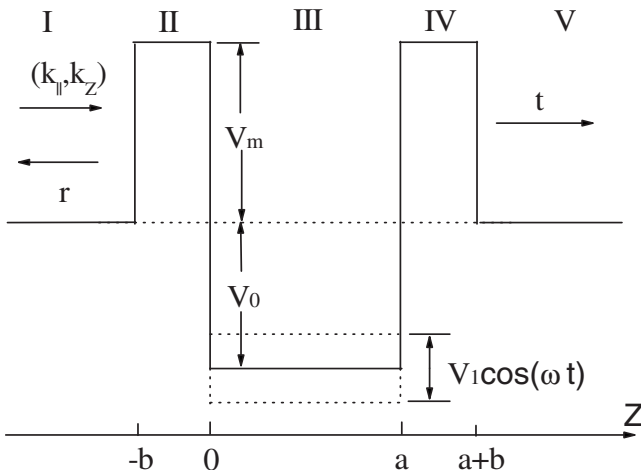


FIG. 1. Potential profile of symmetrical double-barrier structure. V_m is the height of the barriers and V_0 is the depth of the well. a and b are the width of the well and the thickness of the barriers, respectively. $V_1 \cos(\omega t)$ is the oscillatory perturbation applied to the middle well region.

$$\hat{H}_D = \begin{cases} 0, & z \leq -b \text{ and } z \geq a+b \\ \gamma(\hat{\sigma}_x k_x - \hat{\sigma}_y k_y) \frac{\partial^2}{\partial z^2}, & 0 \leq z \leq a \\ 0, & -b < z < 0 \text{ and } a < z < a+b, \end{cases} \quad (4)$$

where γ is the spin-orbit coupling strength in region III (GaSb layer) with $\gamma_1 \approx 0$ and $\gamma_2 \approx 0$ because $\gamma_1 \ll \gamma$ and $\gamma_2 \ll \gamma$ (γ_1 and γ_2 are the spin-orbit coupling strength in GaAs layer and Ga_{0.7}Al_{0.3}As layer, respectively). $\hat{\sigma}_\alpha$ are the Pauli matrices. Inserting $\Phi(z,s,t) = \psi(z,t)\chi_s$ and Eq. (4) into the Schrödinger equation [Eq. (2)], we obtain the electron-spin states of opposite spin polarizations,

$$\chi_{\pm} = \frac{1}{\sqrt{2}} \begin{pmatrix} 1 \\ \mp e^{-i\varphi} \end{pmatrix}, \quad (5)$$

where χ_{\pm} are two pure spinor states and φ denotes the polar angle of the wave vector $\vec{k}_{\parallel} = (k_{\parallel} \cos \varphi, k_{\parallel} \sin \varphi)$ in the xy plane. The orientation of electron spin $\vec{s}_{\pm}(\vec{k}_{\parallel}) = \chi_{\pm}^{\dagger} \hat{\sigma} \chi_{\pm} = (\mp \cos \varphi, \pm \sin \varphi, 0)$ corresponding to the eigenstates χ_{\pm} depends on the direction of the wave vector \vec{k}_{\parallel} . In equilibrium, the momentum distribution of the incident electrons is isotropic in the xy plane and therefore the average spin of the transmitted electrons vanishes.¹⁰ In order to obtain the net spin polarization in the transmitted electrons, we consider the case that the in-plane wave vector of the incident electron is along a fixed direction, for example, $\varphi = 0$, which results completely from an electric field applied along the $-x$ direction. For simplicity, we assume that k_{\parallel} is invariable. In the spin subspace, the Hamiltonian \hat{H} may reduce to

$$\hat{H}_{\pm} = \chi_{\pm}^{\dagger} \hat{H} \chi_{\pm} = -\frac{\hbar^2}{2\mu_{\pm}} \frac{\partial^2}{\partial z^2} + \frac{\hbar^2 k_{\parallel}^2}{2\mu} + V(z,t), \quad (6)$$

where $\mu_{\pm} = \mu(1 \pm \gamma 2\mu k_{\parallel} / \hbar^2)^{-1}$ is the modified effective mass of electron which depends not only on Dresselhaus coupling constant γ and the in-plane electron wave vector k_{\parallel} but also on the orientation of electron spin. Although the modification of the electron effective mass is very small, it plays an important role in generating of the resonance-peak splitting. Using Floquet theory,^{23–25} we obtain the wave function inside the potential well,²⁰

$$\begin{aligned} \Phi_{\pm}^{\text{III}} = & \chi_{\pm} \sum_{n=-\infty}^{+\infty} \sum_{m=-\infty}^{+\infty} [a_m^{\pm} e^{iq_m^{\pm} z} \\ & + b_m^{\pm} e^{-iq_m^{\pm} z}] J_{n-m} \left(\frac{V_1}{\hbar\omega} \right) e^{-iE_{zn}^{\pm} t/\hbar} \exp(i\vec{k}_{\parallel} \cdot \vec{\rho} - iE_{\parallel}^{\pm} t/\hbar), \end{aligned} \quad (7)$$

where a_m^{\pm} and b_m^{\pm} are constant coefficients,

$$q_m^{\pm} = \sqrt{\frac{2\mu_{\pm}}{\hbar^2} \left(E_{z0}^{\pm} + m\hbar\omega + \frac{\hbar^2 k_{\parallel}^2}{2\mu_1} - \frac{\hbar^2 k_{\parallel}^2}{2\mu} + V_0 \right)},$$

and

$$J_{n-m} \left(\frac{V_1}{\hbar\omega} \right)$$

is the Bessel function of the first kind. $\vec{\rho}=(x,y)$ is a vector parallel to the plane of the potential well. The incoming and outgoing waves form the sidebands (or Floquet channels) with energy spacing $\hbar\omega$ according to $E_n^{\pm}=E_F^{\pm}+n\hbar\omega$ (n is the sideband index). The mode of $E_n < 0$ is an evanescent mode, and the corresponding sideband is called an evanescent sideband because such a mode with imaginary k_n cannot propagate.^{26,27}

Since incident electrons will be scattered inelastically into an infinite number of Floquet sidebands inside the potential well, the wave function outside the well can be written as the superposition of waves with all values of energy:

$$\begin{aligned} \Phi_{\pm}^{\text{I}}(z,t) = & \chi_{\pm} \left[e^{ik_{z0}^{\pm} z - iE_{z0}^{\pm} t/\hbar} + \sum_{n=-\infty}^{+\infty} r_{n0}^{\pm} e^{-ik_{zn}^{\pm} z - iE_{zn}^{\pm} t/\hbar} \right] \\ & \times \exp(i\vec{k}_{\parallel} \cdot \vec{\rho} - iE_{\parallel}^{\pm} t/\hbar), \end{aligned} \quad (8)$$

$$\begin{aligned} \Phi_{\pm}^{\text{II}}(z,t) = & \chi_{\pm} \sum_{n=-\infty}^{+\infty} [c_{n0}^{\pm} e^{-k_{zn}^{\pm} z} + d_{n0}^{\pm} e^{k_{zn}^{\pm} z}] e^{-iE_{zn}^{\pm} t/\hbar} \\ & \times \exp(i\vec{k}_{\parallel} \cdot \vec{\rho} - iE_{\parallel}^{\pm} t/\hbar), \end{aligned} \quad (9)$$

$$\begin{aligned} \Phi_{\pm}^{\text{IV}}(z,t) = & \chi_{\pm} \sum_{n=-\infty}^{+\infty} [e_{n0}^{\pm} e^{-k_{zn}^{\pm} z} + f_{n0}^{\pm} e^{k_{zn}^{\pm} z}] e^{-iE_{zn}^{\pm} t/\hbar} \\ & \times \exp(i\vec{k}_{\parallel} \cdot \vec{\rho} - iE_{\parallel}^{\pm} t/\hbar), \end{aligned} \quad (10)$$

$$\begin{aligned} \Phi_{\pm}^{\text{V}}(z,t) = & \chi_{\pm} \sum_{n=-\infty}^{+\infty} t_{n0}^{\pm} e^{ik_{zn}^{\pm} z - iE_{zn}^{\pm} t/\hbar} \exp(i\vec{k}_{\parallel} \cdot \vec{\rho} - iE_{\parallel}^{\pm} t/\hbar), \end{aligned} \quad (11)$$

where

$$\begin{aligned} k_{zn}^{\pm} = & \sqrt{\frac{2\mu_1}{\hbar^2} (E_{z0}^{\pm} + n\hbar\omega)}, \\ k_{zn}^{b\pm} = & \sqrt{\frac{2\mu_2}{\hbar^2} \left(V_m - E_{z0}^{\pm} - n\hbar\omega - \frac{\hbar^2 k_{\parallel}^2}{2\mu_1} + \frac{\hbar^2 k_{\parallel}^2}{2\mu_2} \right)} \end{aligned}$$

, $E_{\parallel}^{\pm} = \frac{\hbar^2 k_{\parallel}^2}{2\mu_1}$, and $E_{z0}^{\pm} + E_{\parallel}^{\pm} = E_0^{\pm}$. We only consider the case that $E_{z0}^{\pm} \in [0, \hbar\omega)$ corresponding to the propagating mode of low-energy. c_{n0}^{\pm} , d_{n0}^{\pm} , e_{n0}^{\pm} , and f_{n0}^{\pm} are the constant coefficients. r_{n0}^{\pm} and t_{n0}^{\pm} are the probability amplitudes of the reflecting

waves and outgoing waves from the sideband 0 to sideband n , respectively. The continuity of Φ_{\pm} and $\frac{1}{\mu} \frac{\partial}{\partial z} \Phi_{\pm}$ at the interfaces $z=-b$, $z=0$, $z=a$, and $z=a+b$ requires

$$e^{-ik_{zn}^{a\pm} b} \delta_{n0} + e^{ik_{zn}^{a\pm} b} r_{n0}^{\pm} = e^{k_{zn}^{b\pm} b} c_{n0}^{\pm} + e^{-k_{zn}^{b\pm} b} d_{n0}^{\pm},$$

$$e^{-ik_{zn}^{a\pm} b} \delta_{n0} - e^{ik_{zn}^{a\pm} b} r_{n0}^{\pm} = \frac{\mu_1 k_{zn}^{b\pm}}{i\mu_2 k_{zn}^{a\pm}} (-e^{k_{zn}^{b\pm} b} c_{n0}^{\pm} + e^{-k_{zn}^{b\pm} b} d_{n0}^{\pm}),$$

$$c_{n0}^{\pm} + d_{n0}^{\pm} = \sum_{m=-\infty}^{+\infty} J_{n-m} \left(\frac{V_1}{\hbar\omega} \right) (a_m^{\pm} + b_m^{\pm}),$$

$$-c_{n0}^{\pm} + d_{n0}^{\pm} = \sum_{m=-\infty}^{+\infty} \frac{1}{k_{zn}^{b\pm}} J_{n-m} \left(\frac{V_1}{\hbar\omega} \right) \frac{i\mu_2 q_m^{\pm}}{\mu_{\pm}} (a_m^{\pm} - b_m^{\pm}),$$

$$\sum_{m=-\infty}^{+\infty} J_{n-m} \left(\frac{V_1}{\hbar\omega} \right) (e^{iq_m^{\pm} a} a_m^{\pm} + e^{-iq_m^{\pm} a} b_m^{\pm}) = e^{-k_{zn}^{b\pm} a} e_{n0}^{\pm} + e^{k_{zn}^{b\pm} a} f_{n0}^{\pm},$$

$$\begin{aligned} \sum_{m=-\infty}^{+\infty} \frac{1}{k_{zn}^{b\pm}} J_{n-m} \left(\frac{V_1}{\hbar\omega} \right) \frac{i\mu_2 q_m^{\pm}}{\mu_{\pm}} (e^{iq_m^{\pm} a} a_m^{\pm} - e^{-iq_m^{\pm} a} b_m^{\pm}) = & -e^{-k_{zn}^{b\pm} a} e_{n0}^{\pm} \\ & + e^{k_{zn}^{b\pm} a} f_{n0}^{\pm}, \end{aligned}$$

$$e^{-k_{zn}^{b\pm} (a+b)} e_{n0}^{\pm} + e^{k_{zn}^{b\pm} (a+b)} f_{n0}^{\pm} = e^{ik_{zn}^{\pm} (a+b)} t_{n0}^{\pm},$$

$$-e^{-k_{zn}^{b\pm} (a+b)} e_{n0}^{\pm} + e^{k_{zn}^{b\pm} (a+b)} f_{n0}^{\pm} = \frac{i\mu_2 k_{zn}^{a\pm}}{\mu_1 k_{zn}^{b\pm}} e^{ik_{zn}^{\pm} (a+b)} t_{n0}^{\pm}. \quad (12)$$

The continuity conditions of the wave functions [Eq. (12)] can be expressed as a compact matrix form,

$$\begin{bmatrix} \mathbf{\Delta} \\ \mathbf{R} \end{bmatrix} = \frac{1}{2} \begin{bmatrix} \mathbf{S}_+ & \mathbf{S}_- \\ \mathbf{S}_+^* & \mathbf{S}_-^* \end{bmatrix} \begin{bmatrix} \mathbf{C} \\ \mathbf{D} \end{bmatrix}, \quad (13)$$

$$\begin{bmatrix} \mathbf{C} \\ \mathbf{D} \end{bmatrix} = \frac{1}{2} \begin{bmatrix} \bar{\mathbf{J}}^* & \bar{\mathbf{J}} \\ \bar{\mathbf{J}} & \bar{\mathbf{J}}^* \end{bmatrix} \begin{bmatrix} \mathbf{A} \\ \mathbf{B} \end{bmatrix}, \quad (14)$$

$$\begin{bmatrix} \mathbf{A} \\ \mathbf{B} \end{bmatrix} = \frac{1}{2} \begin{bmatrix} \mathbf{J}_- & \mathbf{J}_+ \\ \mathbf{J}_+^* & \mathbf{J}_-^* \end{bmatrix} \begin{bmatrix} \mathbf{E} \\ \mathbf{F} \end{bmatrix}, \quad (15)$$

$$\begin{bmatrix} \mathbf{E} \\ \mathbf{F} \end{bmatrix} = \frac{1}{2} \begin{bmatrix} \mathbf{X}_- & \mathbf{X}_-^* \\ \mathbf{X}_+ & \mathbf{X}_+^* \end{bmatrix} \begin{bmatrix} \mathbf{T} \\ \mathbf{O} \end{bmatrix}, \quad (16)$$

where \mathbf{A} , \mathbf{B} , \mathbf{C} , \mathbf{D} , \mathbf{E} , \mathbf{F} , \mathbf{R} , $\mathbf{\Delta}$, \mathbf{T} , and \mathbf{O} are the column matrices with the elements $A_n = a_n^{\pm}$, $B_n = b_n^{\pm}$, $C_n = c_{n0}^{\pm}$, $D_n = d_{n0}^{\pm}$, $E_n = e_{n0}^{\pm}$, $F_n = f_{n0}^{\pm}$, $R_n = r_{n0}^{\pm}$, $\Delta_n = \delta_{n0}$, $T_n = t_{n0}^{\pm}$, and $O_n = 0$. The square matrices \mathbf{S}_{\pm} , \mathbf{X}_{\pm} , $\bar{\mathbf{J}}$, $\mathbf{J}_{\pm} = \mathbf{Q}^{-1}(\mathbf{J}^{-1} + \bar{\mathbf{J}}^{-1})\mathbf{X}_a$, and $\mathbf{J}_- = \mathbf{Q}^{-1}(\mathbf{J}^{-1} - \bar{\mathbf{J}}^{-1})\mathbf{X}_a^{-1}$ are defined by the following matrix elements:

$$S_{+nm} = e^{ik_{zn}^{a\pm} b} \left(1 + \frac{i\mu_1 k_{zn}^{b\pm}}{\mu_2 k_{zn}^{a\pm}} \right) e^{k_{zn}^{b\pm} b} \delta_{nm},$$

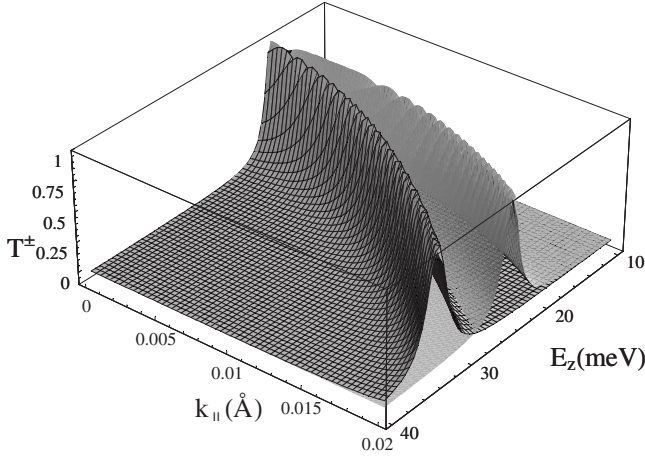


FIG. 2. Splitting of the resonance transmission in the absence of oscillating field for $V_0=200$ meV, $V_m=250$ meV, $a=90$ Å, $b=30$ Å, $\mu_1=0.066m_e$, $\mu_2=0.088m_e$, $\mu_3=0.041m_e$, and $\gamma=1.87 \times 10^5$ meV Å³. The mesh curve corresponds to spin-up electron and smooth curve to spin-down electron.

$$S_{-nm} = e^{ik_{zn}^{a\pm}b} \left(1 - \frac{i\mu_1 k_{zn}^{b\pm}}{\mu_2 k_{zn}^{a\pm}} \right) e^{-k_{zn}^{b\pm}b} \delta_{nm},$$

$$\bar{J}_{nm} = \left(1 + \frac{i\mu_2 q_m^{\pm}}{\mu_{\pm} k_{zn}^{b\pm}} \right) J_{n-m}(V_1/\hbar\omega),$$

$$X_{+nm} = \left(1 + \frac{i\mu_2 k_{zn}^{a\pm}}{\mu_1 k_{zn}^{b\pm}} \right) \exp[(ik_{zn}^{a\pm} - k_{zn}^{b\pm})(a+b)] \delta_{nm},$$

$$X_{-nm} = \left(1 - \frac{i\mu_2 k_{zn}^{a\pm}}{\mu_1 k_{zn}^{b\pm}} \right) \exp[(ik_{zn}^{a\pm} + k_{zn}^{b\pm})(a+b)] \delta_{nm},$$

$$J_{nm} = J_{n-m}(V_1/\hbar\omega),$$

$$\tilde{J}_{nm} = \frac{i\mu_2 q_m^{\pm}}{\mu_{\pm} k_{zn}^{b\pm}} J_{n-m}(V_1/\hbar\omega),$$

$$Q_{nm} = e^{iq_m^{\pm}a} \delta_{nm}, \quad X_{anm} = e^{k_{zn}^{b\pm}a} \delta_{nm}.$$

A straightforward calculation yields the matrix form of the transmission amplitude with the help of Eqs. (13)–(16),

$$\mathbf{T} = 16\mathbf{P}^{-1}\mathbf{\Delta}, \quad (17)$$

with $\mathbf{P} = (\mathbf{S}_+\bar{\mathbf{J}}^* + \mathbf{S}_-\bar{\mathbf{J}})(\mathbf{J}_-\mathbf{X}_- + \mathbf{J}_+\mathbf{X}_+) + (\mathbf{S}_+\bar{\mathbf{J}} + \mathbf{S}_-\bar{\mathbf{J}}^*)(\mathbf{J}_-\mathbf{X}_- + \mathbf{J}_+\mathbf{X}_+)$. The total electron-transmission probabilities of the opposite spin orientations are given by

$$T^{\pm} = \sum_{m=0}^{+\infty} \frac{k_m^a}{k_0} |t_{m0}^{\pm}|^2. \quad (18)$$

We now study numerically the resonance transmission of a single incident electron through a symmetric semiconductor double-barrier structure with Dresselhaus spin-orbit coupling and an oscillating field. The minimum number of sidebands needed in the sum of Eq. (18) depends on the

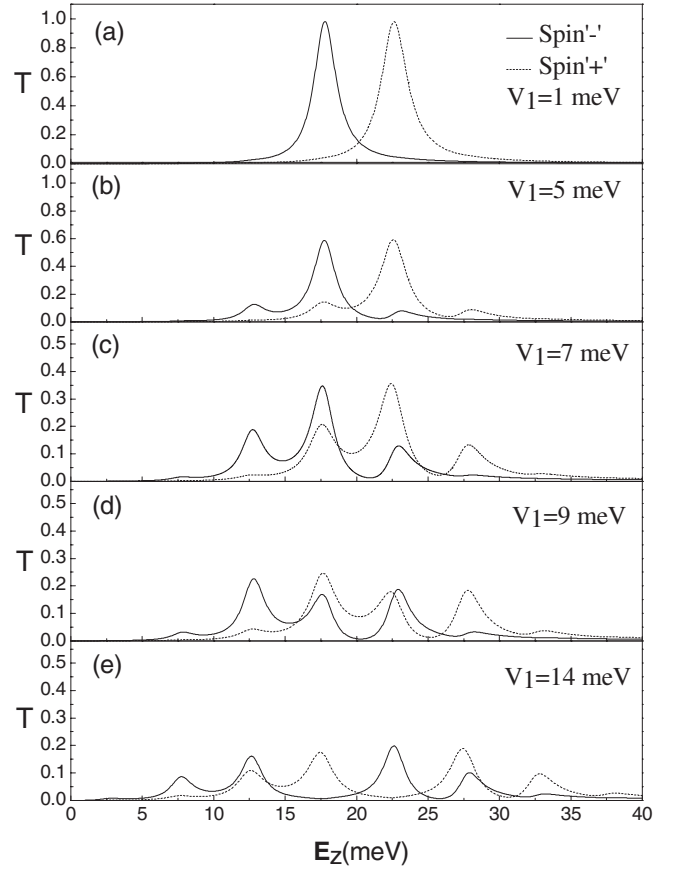


FIG. 3. The transmissivity for spin-up and spin-down electrons versus E_z with $k_{\parallel}=0.01$ Å⁻¹, $\hbar\omega=5$ meV, $V_1=1, 5, 7, 9, 14$ meV, and the other parameters in Fig. 2.

oscillation amplitude of the potential. In general, it is enough to consider the number $N > V_1/\hbar\omega$.

The interaction between the incident electron and the oscillating field leads to photon-mediated resonance transmission which results in the multiplet structure of the transmission coefficients.²⁸ Dresselhaus spin-orbit coupling induces the splitting of the multiplet spectrum, in which in-plane electron wave vector plays an important role. In Fig. 2, we plot the transmission probability as a function of the in-plane electron wave vector k_{\parallel} along the direction of $\varphi=0$ and the energy E_z of the incident electron in the absence of the oscillating field. The transmission spectrum splits into two resonance peaks corresponding to the electrons with opposite spin polarizations. The spacing between two splitting resonance peaks depends on in-plane electron wave vector for a given semiconductor heterostructure. The positions of two resonance peaks shift to the higher energy direction as k_{\parallel} increases, which results from the fact that the effective potential well becomes shallower with increasing k_{\parallel} and thus the quasibound level (above Fermi level) lifts. When an oscillating field is applied in the potential well, the photon-mediated transmission resonances occur. Figure 3(a) shows the transmission resonances for the weak coupling ($V_1=1$ meV) between the electron and field similar to the case in Fig. 2. The quasibound levels for spin-up and spin-down electrons are $E_q^+=22.6$ meV and $E_q^-=17.8$ meV, respectively,

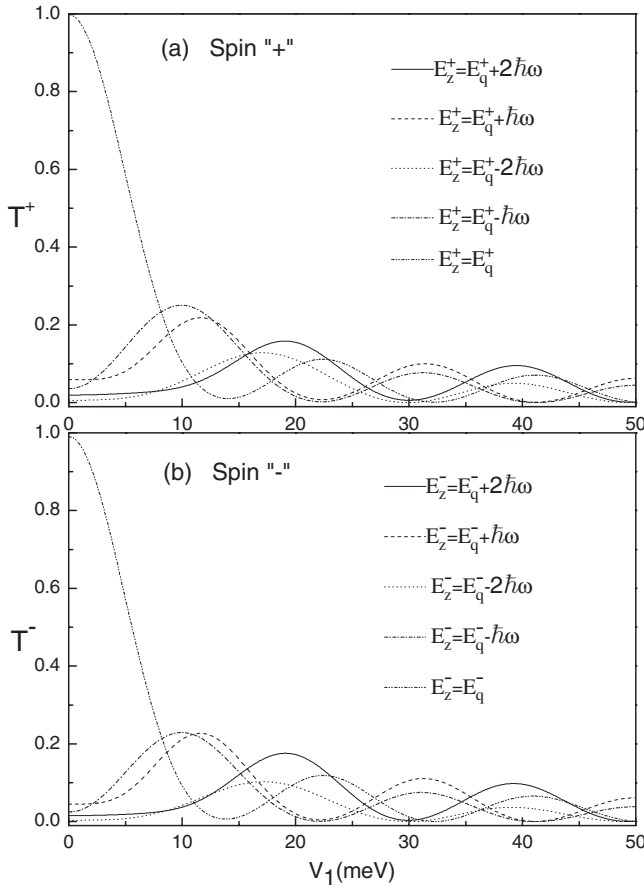


FIG. 4. The transmissivity as a function of the amplitude of oscillating field for $k_{\parallel}=0.01 \text{ \AA}^{-1}$, $\hbar\omega=5 \text{ meV}$, $E_z^{\pm}=E_q^{\pm}$, $E_q^{\pm}\pm\hbar\omega$, $E_q^{\pm}\pm 2\hbar\omega$, and the other parameters in Fig. 2.

corresponding to the positions of two splitting peaks. With the increasing amplitude of the applied oscillating field, the multiplet structure of transmission spectrum occurs and the central peak decreases progressively. Figure 3(b) shows one-photon process for $V_1=5 \text{ meV}$ and $\hbar\omega=5 \text{ meV}$, in which an incident electron of energies $E_z^{\pm}=E_q^{\pm}-\hbar\omega$ (or $E_z^{\pm}=E_q^{\pm}+\hbar\omega$) absorbs (or emits) a photon exciting to the quasibound level, and, consequently, the lateral peaks occur as shown in Fig. 3(c) for $V_1=7 \text{ meV}$. The two-photon process takes place by two-photon absorption ($E_z^{\pm}=E_q^{\pm}-2\hbar\omega$) or emission ($E_z^{\pm}=E_q^{\pm}+2\hbar\omega$). The left-end and right-end small peaks in Fig. 3(d) correspond to the two-photon process for $V_1=9 \text{ meV}$ and the central peak is lower than the lateral peaks. When V_1 increases to 14 meV , the lateral peaks are dominant and the central peak disappears [see Fig. 3(e)]. For a given semiconductor heterostructure, the position of the central peak depends on the in-plane electron wave vector k_{\parallel} and the positions of the lateral peaks are determined by k_{\parallel} and the oscillating frequency of the applied field ω . However, their intensities are determined only by the field parameters V_1 and ω . Figure 4 shows the transmission probability as a function of V_1 for $\hbar\omega=5 \text{ meV}$, which varies quasiperiodically with increasing V_1 . The phase of one-photon process is almost opposite to that of two-photon process for the high field amplitude.²⁹

In Fig. 3, it is more interesting to see that the position of

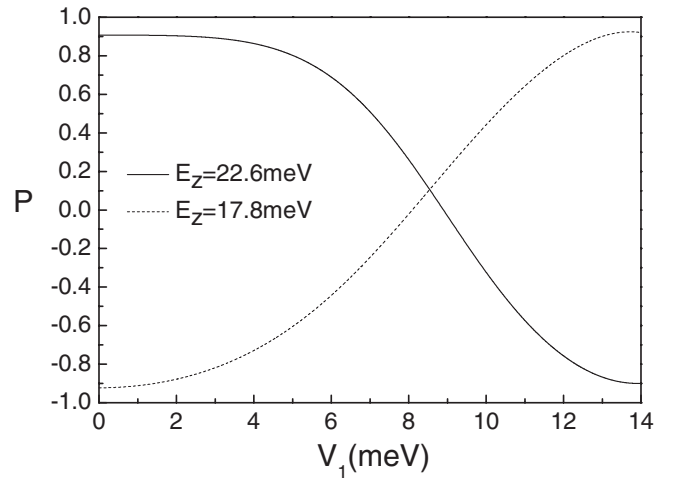


FIG. 5. Spin polarization as a function of the amplitude of oscillating field for $E_z=22.6 \text{ meV}$, 17.8 meV , $k_{\parallel}=0.01 \text{ \AA}^{-1}$, $\hbar\omega=5 \text{ meV}$, and the other parameters in Fig. 2.

the left (or right) lateral peak of spin “+” (or “-”) in one-photon process coincides with that of the central peak of spin - (or +). When V_1 increases from 0 to 14 meV , the central peak of spin - (or +) decreases from the maximum to zero; contrarily, the left (or right) lateral peak of spin + (or -) changes from zero to a finite value, which provides a possibility of controlling the spin polarization of the transmitting electrons with an applied field. The spin polarization of transmitting electrons as a function of the field amplitude V_1 is shown in Fig. 5 according to $P=(T^+-T^-)/(T^++T^-)$ for the incident electron with energies $E_z=17.8$ and 22.6 meV which are the quasibound levels for spin-up and spin-down electrons and may be changed by a gate voltage (included in V_0 in our model). When V_1 increases from 0 to 14 meV , the spin polarization changes from -0.9 to $+0.9$ for the incident electron of energy $E_z=17.8 \text{ meV}$ (from $+0.9$ to -0.9 for $E_z=22.6 \text{ meV}$). The characteristics of transmission spectrum suggest that one can exploit the splitting of the multiplet spectrum as the basis of a spin-polarization modulator and control the spin polarization of the current.

For a very narrow potential well, the quasibound levels disappear and the resonance tunneling via the quasibound levels cannot take place. However, the electron tunneling through the first barrier may emit a photon dropping to the bound state (bound level $E_b < 0$) and is then excited back to the original state by absorbing a photon to tunnel through the second barrier. The photon-mediated tunneling is shown in Fig. 6 for different V_1 . The asymmetric line shape in Fig. 6 is the typical characteristic of Fano resonance. The position of the transmission-probability peak is determined by $\hbar\omega=E_z-E_b$. The width of transmission-probability peak depends on the amplitude of the field V_1 proportional to the coupling strength between electron and field which leads to the broadening of the energy level. The insets of Fig. 6 correspond to the spin polarization as a function of the incident energy. For example, the spin polarization is about 90% for $V_1=20 \text{ meV}$, while it can approach to 95% (for the energy E_z from 1 to 3.5 meV) and even 99% (for the energy E_z from 3.5 to 4.5 meV) with a smaller value of the field amplitude

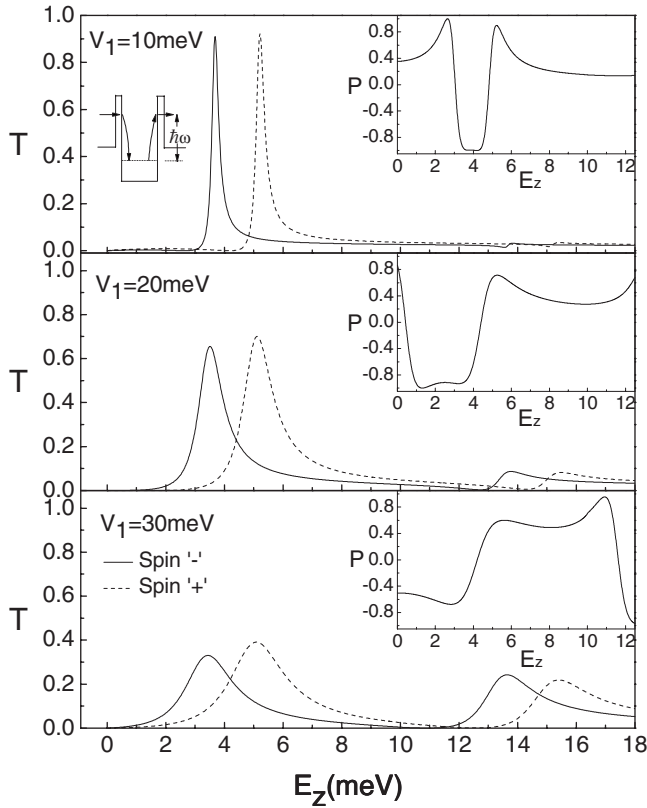


FIG. 6. The transmissivity of photon-mediated tunneling through double-barrier via bound level in well for $a=30 \text{ \AA}$, $b=25 \text{ \AA}$, $k_{\parallel}=0.02 \text{ \AA}^{-1}$, $\hbar\omega=10 \text{ meV}$, $V_1=10, 20, \text{ and } 30 \text{ meV}$, and the other parameters in Fig. 2. The insets are the corresponding spin polarization.

$V_1=10 \text{ meV}$. It is apparent that this spin filtering occurs due to the fact that the energy window for the electrons of spin states $+$ is almost closed with respect to the electrons of spin states $-$ and vice versa.

The spin filtering mechanism for the electrons tunneling via the quasibound state is similar to that explained in Ref.

11. However, for a narrow well in the absence of the quasi-bound state, the sharp Fano resonance induced by the bound state results in higher spin filtering capability. The large spin polarization occurs in the energy window between the resonance and associated antiresonance (Fig. 6), in agreement with the observation in Ref. 30. Since the energy separation between the resonance and antiresonance depends on the oscillating field in the potential well, the energy window width of the large spin polarization in our model can be controlled by the applied field, which is essentially different from other schemes. It is not difficult to experimentally implement this proposal with the technology of the high-precision epitaxial semiconductor growth.³¹

In summary, we have studied the electron transmission through a symmetric double-barrier structure with Dresselhaus spin-orbit coupling in the presence of an oscillating field applied to the potential-well region. Dresselhaus spin-orbit coupling eliminates the spin degeneracy and results in the spin splitting, which is determined by the in-plane wave vector \vec{k}_{\parallel} for a given double-barrier structure. The multiplet structure in the transmission spectrum appears and splits into two sets due to the multiphoton process. The number of the resonance peaks in the multiplet spectrum and the distance between the adjacent peaks can be controlled by adjusting the amplitude and the frequency of the external oscillating field, respectively. It is interesting to observe the position overlap between the left (or right) lateral peak of spin $+$ (or $-$) and the central peak of spin $-$ (or $+$), as well as the V_1 dependence of resonance peaks, which may provide a possibility of controlling the spin polarization of the transmitting electrons with an applied field. For the narrow well case, the asymmetric line shape of Fano resonance in the transmission probability due to the interference between the photon-mediated transition via the bound state and the direct tunneling results in the large spin polarization.

This work was supported by the National Natural Science Foundation of China (Grant No. 10475053) and Shanxi Natural Science Foundation (Grant No. 20051002).

*nieyh@sxu.edu.cn

¹E. Y. Tsymlal, O. N. Mryasov, and P. R. LeClair, *J. Phys.: Condens. Matter* **15**, R109 (2003).
²R. H. Silsbee, *J. Phys.: Condens. Matter* **16**, R179 (2004).
³I. Žutić, J. Fabian, and S. Das Sarma, *Rev. Mod. Phys.* **76**, 323 (2004).
⁴A. Voskoboynikov, S. S. Lin, C. P. Lee, and O. Tretyak, *J. Appl. Phys.* **87**, 387 (2000).
⁵D. Z.-Y. Ting and X. Cartoixa, *Appl. Phys. Lett.* **81**, 4198 (2002).
⁶T. Koga, J. Nitta, H. Takayanagi, and S. Datta, *Phys. Rev. Lett.* **88**, 126601 (2002).
⁷C.-E. Shang, Y. Guo, and X.-Y. Chen, *J. Appl. Phys.* **96**, 3339 (2004).
⁸K. C. Hall, W. H. Lau, K. Gündoğdu, M. E. Flatte, and T. F. Boggess, *Appl. Phys. Lett.* **83**, 2937 (2003).
⁹S. A. Tarasenko, V. I. Perel', and I. N. Yassievich, *Phys. Rev. Lett.*

93, 056601 (2004).

¹⁰V. I. Perel', S. A. Tarasenko, I. N. Yassievich, S. D. Ganichev, V. V. Bel'kov, and W. Prettl, *Phys. Rev. B* **67**, 201304(R) (2003).
¹¹M. M. Glazov, P. S. Alekseev, M. A. Odnoblyudov, V. M. Chistyakov, S. A. Tarasenko, and I. N. Yassievich, *Phys. Rev. B* **71**, 155313 (2005).
¹²A. Voskoboynikov, S. S. Liu, and C. P. Lee, *Phys. Rev. B* **59**, 12514 (1999).
¹³E. A. de Andrada e Silva and G. C. La Rocca, *Phys. Rev. B* **59**, R15583 (1999).
¹⁴P. R. Hammar and M. Johnson, *Appl. Phys. Lett.* **79**, 2591 (2001).
¹⁵A. T. Hanbicki, B. T. Jonker, G. Itskos, G. Kiioseoglou, and A. Petrou, *Appl. Phys. Lett.* **80**, 1240 (2002).
¹⁶G. Dresselhaus, *Phys. Rev.* **100**, 580 (1955).
¹⁷G. Schmidt, D. Ferrand, L. W. Molenkamp, A. T. Filip, and B. J.

- van Wees, Phys. Rev. B **62**, R4790 (2000).
- ¹⁸E. I. Rashba, Phys. Rev. B **62**, R16267 (2000).
- ¹⁹Xue-Hua Wang, Ben-Yuan Gu, and Guo-Zhen Yang, Phys. Rev. B **55**, 9340 (1997); E. A. de Andrada e Silva, G. C. La Rocca, and F. Bassani, *ibid.* **55**, 16293 (1997).
- ²⁰Cun-Xi Zhang, Y.-H. Nie, and J.-Q. Liang, Phys. Rev. B **73**, 085307 (2006).
- ²¹H. J. Reittu, J. Phys.: Condens. Matter **6**, 1847 (1994).
- ²²H. B. de Carvalho, Y. Galvão Gobato, M. J. S. P. Brasil, V. Lopez-Richard, G. E. Marques, I. Camps, M. Henini, L. Eaves, and G. Hill, Phys. Rev. B **73**, 155317 (2006).
- ²³J. H. Shirley, Phys. Rev. **138**, B979 (1965).
- ²⁴M. Holthaus and D. Hone, Phys. Rev. B **47**, 6499 (1993).
- ²⁵T. Fromherz, Phys. Rev. B **56**, 4772 (1997).
- ²⁶W. Li and L. E. Reichl, Phys. Rev. B **60**, 15732 (1999).
- ²⁷P. F. Bagwell and R. K. Lake, Phys. Rev. B **46**, 15329 (1992).
- ²⁸C. P. del Valle, R. Lefebvre, and O. Atabek, Phys. Rev. A **59**, 3701 (1999).
- ²⁹W. Cai, P. Hu, T. F. Zheng, B. Yudanin, and M. Lax, Phys. Rev. B **41**, 3513 (1990).
- ³⁰T. Sandu, A. Chantis, and R. Iftimie, Phys. Rev. B **73**, 075313 (2006).
- ³¹R. K. Hayden, A. E. Gunnaes, M. Missous, R. Khan, M. J. Kelly, and M. J. Goringe, Semicond. Sci. Technol. **17**, 135 (2002).